

Scattering of hyperthermal effusive N and N₂ beams at metal surfaces

Michael A. Gleeson¹, Hirokazu Ueta^{1,*} and Aart W. Kleyn^{1,2,3}

¹ FOM Institute DIFFER (Dutch Institute For Fundamental Energy Research), Postbox 1207, 3430 BE Nieuwegein, The Netherlands

² Van 't Hoff Institute for Molecular Sciences, Faculty of Science, University of Amsterdam, The Netherlands

³ Leiden Institute of Chemistry, Leiden University, The Netherlands

* present address: Laboratoire de Chimie-Physique Moléculaire, Ecole Polytechnique Fédérale de Lausanne, Lausanne, Switzerland

Abstract

Molecular beam experiments with specially prepared beams allow the study of the interaction of very reactive species at surfaces. In the present case the focus is primarily on the interaction of N-atoms with surfaces. In this chapter questions that will be addressed include:

- What is the scattering pattern and energy transfer of N-atoms at surfaces?
- Can adsorption of N-atoms lead to a passive layer that is not reactive to incident N-atoms?
- Conversely, can N-atoms remove N-atoms in an Eley-Rideal or hot atom reaction?
- Does the electronic state of the atoms matter?
- Can the interaction already be described by state-of-time art theory?

The methods used will be introduced with examples of fast Ar scattering from Ag(111). Subsequently, the interaction of N-atoms with Ag(111) and Ru(0001) will be discussed in order to address the questions listed above. Some work with N₂ will also be shown.

Keywords: *hyperthermal, molecular beam, translational energy, Eley-Rideal reaction, surface scattering, potential (surfaces), corrugation, Ag, Ru, DFT, electronic (state), energy transfer, passivation.*

Introduction

The fate of a chemical reaction is often determined by the availability of energy and the reactivity of the species involved. Energy, both translational and internal, can allow the reactants to overcome activation barriers and possible endoergicity of the reaction. The most probable path on the potential energy surface describing the reaction is thus governed by availability of energy. Working with excess translational energy limits reaction yields but allows exploration of the nature of the potential energy surfaces involved. Scattering experiments were built to carry out such studies both in gas-phase collisions and in atom/molecule surface collisions. In this chapter we focus on the latter case for experimental studies involving reactive atoms and molecules and we compare these results to similar studies with inert noble gas atoms for calibration.

The importance of surface scattering experiments was already realized in the 1970's [1-4]. From the early work two regimes are identified and the corresponding terms thermal scattering and structure scattering were coined. In the first case the processes are dominated by an energy constraint and the thermal energy of the surface is an important parameter. In addition, parallel momentum conservation applies. In the second case the dynamics at the surface is determined by the potential hyper-surfaces and the surface structure. Collisions are not constrained by the lack of energy and can be seen as one or more binary collisions that are approximately independent. In this case parallel momentum conservation does not apply. Comparing results from the two regimes can give insight into the interaction dynamics as a whole. It turned out that the transition between the two regimes was at a few electronvolt of translational energy. Above this energy the possible energy uptake from the surface motion becomes very small compared to the initial translational energy. The only remaining effect of the thermal motion of the surface is the displacement of the surface atoms from their equilibrium positions. This has a blurring effect on the angular distributions of particles scattered at the surface. In the realm of structure scattering the effect of the gas-surface interaction potential becomes much more visible in the scattering patterns. Effects like surface rainbow scattering become visible in this domain [5]. Most of the studies in this field have been performed using scattering of noble gas atoms.

When studying reactive particles the interaction becomes more complex than for noble gas scattering because there can be a strong attractive force between projectile and surface. The corresponding chemisorption well blurs the difference between thermal and structure scattering, because the potential well accelerates the incoming particles. This effect has been seen for scattering of molecules such as NO or CO from surfaces at which they have a deep chemisorption well. Most studies with reactive atoms have been carried

out with alkali atoms, though mostly at energies well above 10 eV [5, 6]. Studies with fast O- or F-atoms have also been carried out [7-10].

Studies with fast N-atoms are very rare, due to the difficulty to make fast beams of these atoms. Dissociation of N₂ is the most direct way to make N-atom beams, but this is non-trivial because of the large dissociation energy of about 10 eV. In this work we utilize an atmospheric plasma arc to produce a nitrogen beam that contains a mixture of N-atoms and N₂ molecules. Other methods to make fast beams are laser detonation or charge exchange [11-13].

The interaction of N-atoms with surfaces is interesting because nitrides are very stable surfaces with desirable properties. This is due to the very high binding energy of the N-atoms to metal surfaces resulting in stable compounds, for instance for use in silicon or fusion technology, see e.g. [14-16]. To the knowledge of the authors very few studies have been carried out on the interaction of fast N-atoms and surfaces.

N-atoms have low lying excited states that can be populated in molecular beams [17-19]. Excitation or de-excitation of those states makes it possible to study electronically non-adiabatic processes at surfaces. Such processes have been studied extensively at energies of tens of eV's for charge transfer processes at surfaces such as neutralization of protons, noble gas ions, alkali atoms and several molecular ions [6, 8, 9]. The connection of those studies to the lower energy work has been underestimated, see e.g. [20]. Recently, non-adiabatic processes in atom or molecule-surface collisions are studied with great success in experiments using Schottky diodes with ultrathin metal films [21], and using laser prepared vibrationally excited molecular beams [22, 23]. These experiments have also triggered new theoretical methods for the treatment of electronically non-adiabatic processes [24-26].

The ground state interaction of N-atoms and N₂-molecules with metal surfaces is currently being studied by density functional Theory (DFT) methods by a number of groups, see e.g. [27-36]. Such studies yield potential energy hyper-surfaces describing the interaction. The actual interaction dynamics can be studied separately if the processes are electronically adiabatic and the Born-Oppenheimer approximation is valid. Interactions with excited state particles still pose a formidable challenge for theoretical analysis. The structure of the N-containing surfaces is not in all cases known. For Ag(111) the knowledge is summarized in [37] and is limited. For Cu and Ru more is known [38-43]. In general, the N-atoms reside in three fold hollow sites and are almost inside the metal lattice. Their presence can give rise to restructuring and loss of long range order of the surface.

The control of reactant energy and internal state needed for the experiments discussed can be achieved by molecular beam techniques. The technique itself is very well established [44]. Using these techniques we have recently studied the interactions of fast argon atoms, and atomic nitrogen radicals and molecules with metal surfaces. Energies in the 3-6 eV range have been achieved. In addition, a number of other groups have created such hypertermal beams of, for instance, O-atoms, in fact with a sharper energy distribution. These results will be briefly reviewed.

In our studies with reactive nitrogen atoms we investigated their adsorption and scattering from Ag and Ru surfaces, and their interaction with pre-adsorbed nitrogen atoms. The interaction for these strong chemisorption systems is very different as compared to physisorption systems. This is apparent from the energy transfer and angular scattering distributions. It is very noteworthy that pre-coverage of the surface with N-atoms does not significantly alter the dynamics, contrary to expectation. In addition, evidence for strong non-thermal and direct chemistry is observed. It has been determined that the incident beam contains a fraction of excited N-atoms. The first observations of the possible role of these excited atoms have been made.

A surprise was seen in the scattering of fast (6 eV) N₂ from N-covered Ru(0001). Whereas the Ru system exhibited thermal-like scattering at low energies, the angular distribution for fast N₂ from N-Ru was extremely broad, indicating that the addition of N atoms induces significant roughening and disorder of the surface and/or that above a certain threshold energy the surface turns very corrugated and reactive.

At lower energies the interaction between N₂ and surfaces has been studied also with state resolved methods. It was shown that even though the interaction is purely repulsive significant rotational excitation can be observed. For collisions between fast N₂ and Ag(111) beautiful rotational rainbow structures and alignment has been observed [45-48]. In such experiments the dynamics has been determined with a very high level of detail.

Experimental

The measurements relating to the interaction of argon and nitrogen with silver and ruthenium surfaces that are discussed in this text were collected in a plasma beam scattering apparatus [49-51]. It consists of a triply differentially-pumped beam line connected to a UHV scattering chamber. Figure 1 shows a schematic illustration of a vertical cross-section of this beam line and the associated samples chamber.

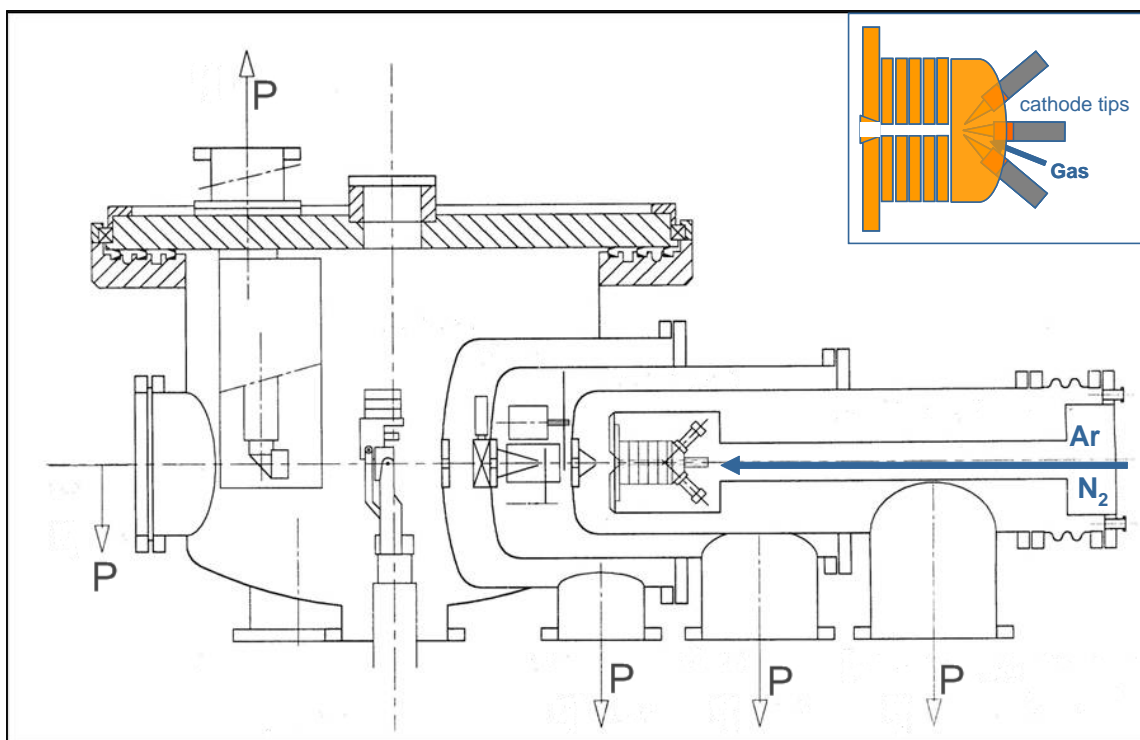


Figure 1: Vertical cross-section of the experimental set-up utilized for the study of the interactions of hypertermal argon and nitrogen with Ag(111) and Ru(0001). Inset: illustration of the configuration of the cascaded arc source.

Starting from the right-hand-side in figure 1, the first stage of the beam line contained an expanding thermal plasma (cascaded arc) source [52, 53]. This source produces a wall-stabilized high-density linear plasma. Plasma is generated by discharge at three symmetrically-mounted cathode tips and transported through a channel in a stack of floating, mutually-isolated plates before expanding into the first vacuum stage of the beam line. In the current case, the channel diameter was 2.5 mm, five plates were used in the channel stack, and the arc was made of copper with tungsten cathode tips. Plasma

particles are sampled from the expansion of the cascaded arc by a grounded, water-cooled copper skimmer with an opening diameter of 0.5mm.

Particles that pass the first skimmer enter the second stage of the beam line. This contains a chopper that is used to produce a pulsed beam, a beam flag for controlled blocking/unblocking of the beam path to the sample, and a pair of deflection plates that allows for deflection of charged particles from the beam. Typically measurements are performed in time-of-flight (TOF) mode, which allows for simultaneous monitoring of both the intensity and energy distributions of scattered particles. A double slit 0.5% duty cycle chopper was employed for this purpose and the pulse frequency was typically 400 Hz. A second skimmer at the entrance from this section to the third stage of the beam line ensures the formation of a well-collimated beam. The aperture of this skimmer is 1 mm in diameter.

The sole function of the third stage is as a buffer chamber ensuring that a low pressure can be maintained in the main (scattering) chamber during operation of the cascaded arc source. It contains an in-vacuum valve that allows for isolation of the high/ultra-high vacuum sections from the medium/low vacuum sections.

The sample is mounted in the centre of the scattering chamber on a three-axis goniometer [54]. The main diagnostic tool is a differentially-pumped quadrupole mass spectrometer (QMS) that can be rotated around the sample to detect particles leaving from the surface along in-plane scattering directions. In combination with the motion of the manipulator, it is possible to directly measure the incident beam and the scattered particles for a large range of incident angle. For presentation of data in this chapter, the incident angle (Θ_i) and outgoing angle (Θ_f) are defined with respect to the surface normal, while the total scattering angle (Θ_t) is defined as $(180^\circ - (\Theta_i + \Theta_f))$. For details of the sample cleaning, characterization, and preparation methods, the reader is referred to the relevant published work for Ag(111) [51, 55] and Ru(0001) [56, 57].

All TOF data points shown in this paper were derived from individual TOF measurements after application of corrections for instrumental time delays and flight time of the ions through the QMS. The latter correction was based on flight times derived from simulation performed using SIMION. Additionally, in the case of N atoms the raw TOF data was corrected for the contribution from N₂ cracking in the QMS ionizer. The incident particle energy, final energies as a function of scattering angle, and angular intensity distributions were all derived from TOF measurements after fitting with shifted Maxwell-Boltzmann (MB) distributions convoluted over the finite chopper opening time and over the spread of arrival times of particles at the surface [58, 59].

Note that the cascaded arc beam line in its current configuration produces particles with average energies $\langle E_i \rangle$ typically in the range of 4-6 eV. Furthermore the beams have a very broad energy distribution, with full-width at half-maximum values (E_{FWHM}) greater than $\langle E_i \rangle$. Figure 2 shows the energy distributions measured for Ar particles from a pure argon plasma and for N and N₂ particles from a pure nitrogen plasma.

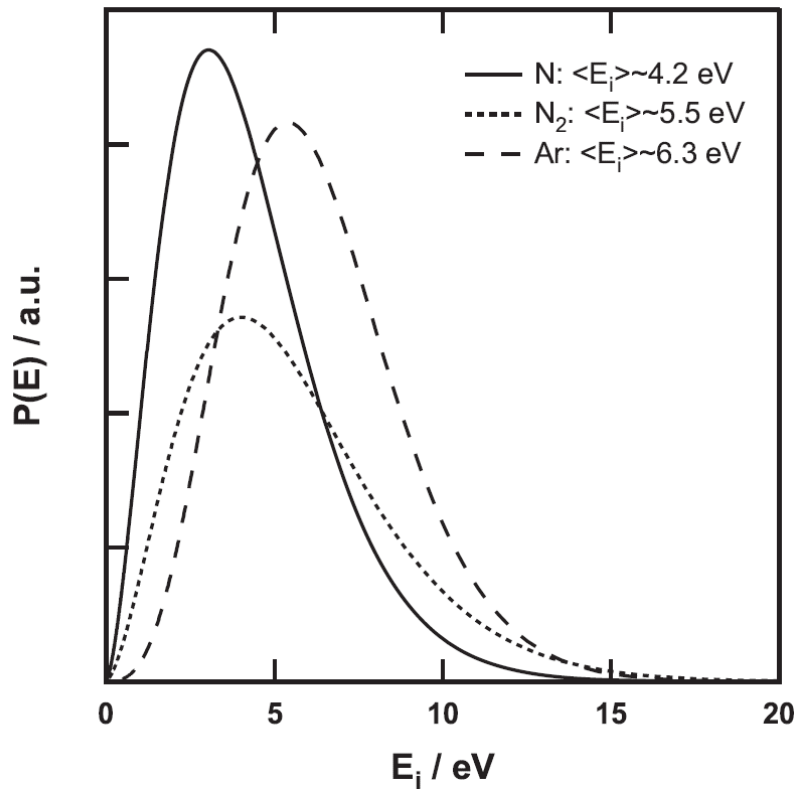


Figure 2: Typical energy distributions of Ar, N and N₂ in the direct beams produced by the cascaded arc source.

N-atom scattering at bare Ag(111)

Scattering at surfaces gives information on the nature of the gas-surface interaction. For the case at hand, it is illustrative to compare scattering of N-atoms to that of Ar from the same surface. A comparison of the angular intensity distributions for beams of fast Ar and N with $\langle E_i \rangle$ of around 5 eV scattered from a bare Ag(111) surface for $\Theta_i=60^\circ$ is shown in figure 3(a). The surface temperature (T_s) was maintained at 600 K by radiative heating during the measurements. It is known that at temperatures ≥ 500 K the nitrogen does not chemisorb at the surface [37]. The incident N atoms can adsorb at the surface but due to the high surface temperature they will quickly recombine and desorb. A theoretical study has indicated that at the present beam energy even temporary trapping in the chemisorption well is unlikely [60]. Note that both the N intensities (left-hand ordinate) and Ar intensities (right-hand ordinate) are normalized relative to their respective intensities in the direct beam. Since the Ar atoms are confined to a comparatively narrow scattered angle range, their relative intensities are significantly higher than those of the scattered N-atoms.

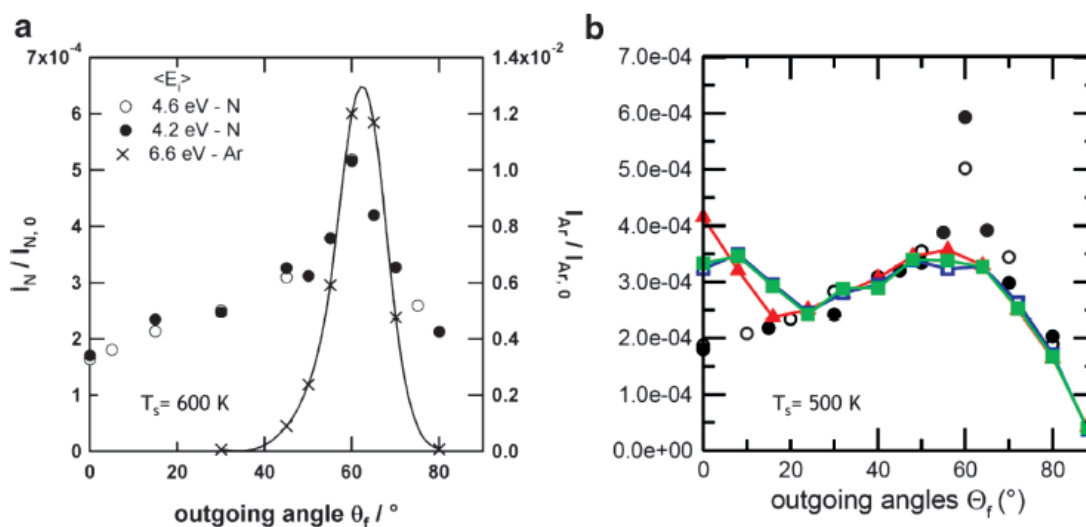


Figure 3: (a) Angular intensity distributions of Ar and N atoms scattered from a bare Ag(111) surface at $\Theta_i=60^\circ$ and $T_s = 600$ K. (b) Comparison of the experimentally measured angular distribution of N atoms scattered from a bare Ag(111) surface at $\Theta_i=60^\circ$ and $T_s = 500$ K with classical trajectory modeling for a rigid surface (red trace), a thermally moving surface (blue trace) and a thermally moving surface with electronic friction (green trace).

The angular distribution of Ar is typical for scattering in a system dominated by van der Waals forces. It is in the transition between thermal scattering and structure

scattering. For Ar scattering from Ru, the other surface discussed at the end of this chapter, structure scattering already appears at these energies [57, 61]. Near-specular reflection occurs with a peak relative reflection intensity of about 0.012 with respect to the primary beam intensity. Such scattering patterns have been seen before for a number of noble gas atoms reflecting at close packed metal surfaces. The angular distribution has not been integrated to confirm that indeed all of the primary beam intensity is recovered in the angular distribution. Since the angular acceptance width of the detector is $\sim 1.6^\circ$ in the scattering plane, finer measurements would be necessary for a reliable determination. More importantly, the angular distribution out of the scattering plane is not measurable in the current set-up. Earlier work at lower energies has indicated that the in-plane and out-of plane angular width are comparable [62]. With this assumption, it is not unreasonable to assume that indeed all Ar from the primary beam is scattered into the specular peak observed.

The angular distribution of the N-atoms shown in figure 3(a) is distinctly different from that of Ar. A very broad distribution is observed with a peak at the specular angle. This pattern is more connected to structure scattering. The peak relative reflection intensity is about 0.0005 with respect to the primary beam intensity. This is a decrease of a factor of 25 with respect to Ar. Again a full integration of all scattered signal is not possible, but it is very reasonable that the dramatic increase of the width of the in-plane distribution leads to the observed decrease of the relative reflection probability in the specular peak. In fact, in the case of N scattering there is only a small preference for specular scattering. Decreasing Θ_i to 40° (results shown in [51]) leads to a broadening of the specular peak for Ar, as expected. For N-atoms the peak at the specular angle almost disappears.

As noted by Ueta *et al.* [51], the angular distributions of N-atoms shown in figure 3 appears to be the result of two distinct distributions: an ‘Ar-like’ specular peak and a very broad distribution in addition. No consistent argumentation could be found for attempts to attribute the two distributions to different physical processes in scattering of ground state N-atoms. In addition, recent theoretical calculations by Martin-Gondre *et al.* [60] show a very good reproduction of the broad part of the spectrum, but missing the specular peak, as shown in figure 3(b). For these calculations, a sophisticated interaction potential between ground state N(⁴S) and the Ag(111) surface has been derived by DFT and it has been parameterized in closed analytical form. Using this potential, classical trajectory scattering calculations have been performed. In these calculations, the energy exchange with the surface has been computed using three different models. It is surprising to see that for a rigid surface, a thermally moving surface (GLO) and a thermally moving surface combined with electronic friction for the N-atom

(LDFFA+GLO) the angular distributions are very similar. The distribution is clearly dominated by structure scattering from the corrugation of the potential energy surface. This corrugation is manifested in figure 4, where potential energy contours are shown for a cross-section running parallel to the close-packed atomic rows and crossing over the hcp three-fold hollow site [60].

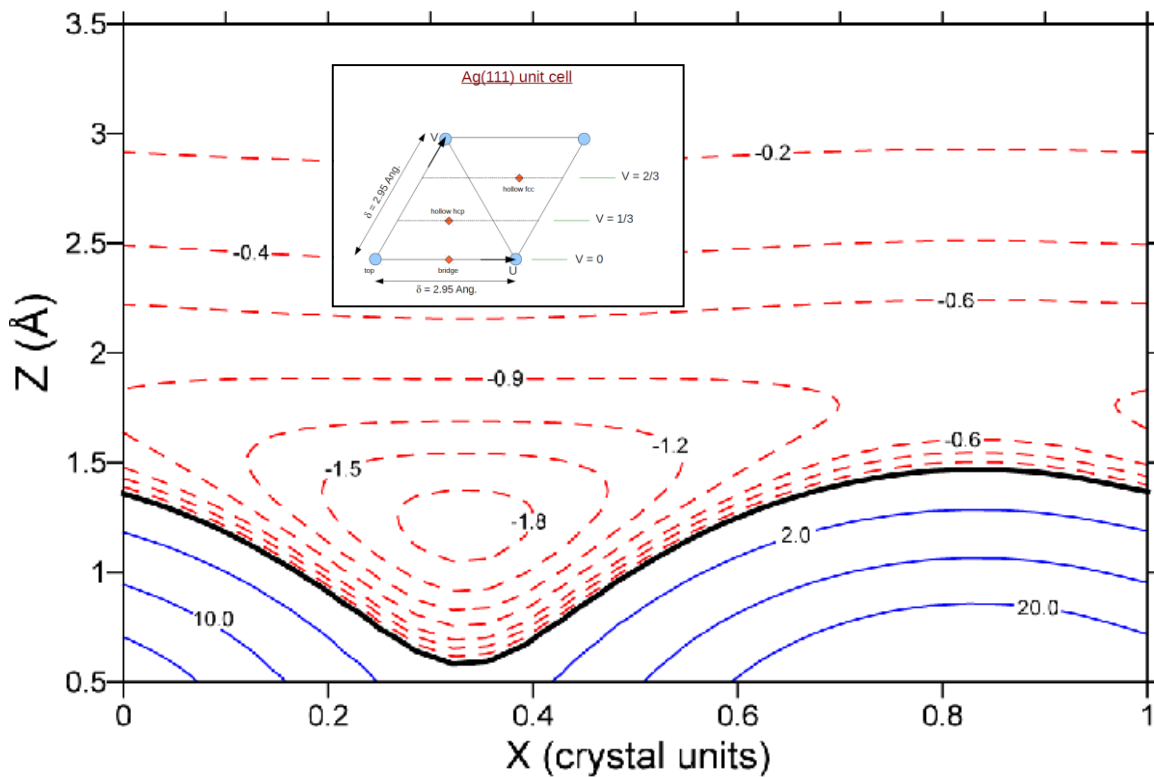


Figure 4: Contour plot of the potential energy surface of the N/Ag(111) system for a cross-section along the $v=1/3$ line indicated on the unit cell.

On the scale of this figure, the contours of the potential energy surface for the interaction between Ar and Ag(111) at energies around 1-5 eV are almost flat as shown in [63, 64]. This difference between N and Ar is well reflected in the angular distributions. The absence of the specular peak in the calculations for N-atom scattering from Ag(111) is to be expected. The potential energy surface in figure 4 shows a very deep chemisorption well and consequently a very corrugated repulsive potential. This gives rise to structure scattering in many directions because parallel momentum is not conserved in collisions involving such a corrugated potential. It is parallel momentum conservation that gives rise to the strong specular peak for Ar scattering. Unless we assume that the DFT potential surface is quite incorrect, for which there are no indications, we have to conclude from the comparison between experiments and

theoretical results in figure 3(b) that there is an ingredient in the physics that the above approach overlooks.

Ueta *et al.* suggest that this missing component might be the presence of excited N-atoms (²P and ²D) in the beam. It is well known that atom sources can deliver such excited atoms, which have long lifetimes [17-19]. Indeed, excited state atoms have been detected during analysis of the primary N-atom beam using Threshold Electron Appearance Potential measurements with the mass spectrometer detector of the system. Figure 5 shows a plot of the N signal measured in the direct beam as a function of the energy of the ionizing electrons in the near-threshold region. The dashed lines indicate the ionization energy of N atoms in the (²P), (²D), and (⁴S) states. As the electron impact energy is increased, there is a distinct increase in the detected intensity at energies less than that required to ionize ground-state N(⁴S) atoms. This signal can only arise from the presence of excited N atoms in the direct beam. The amount of excited atoms has been estimated as a few percent of the total intensity, although a detailed quantification has not been performed. In this case, and in light of the results of the DFT calculations for ground-state N, then we have to consider that the specular peak in the N-atom signal is due to scattering of excited atoms.

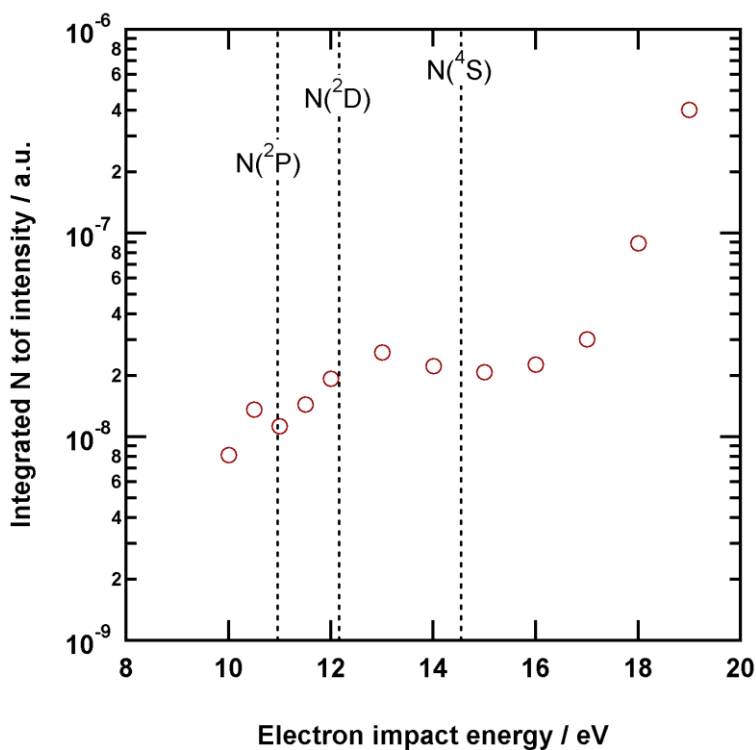


Figure 5: N intensity in the direct beam detected by the QMS as a function of the energy of the ionizing electrons.

Due to the low intensity, it was not possible to determine if the scattered N-atoms were in the ground or an excited state. Further experiments are clearly needed to resolve this conclusively. Nevertheless, we can speculate about the origin of the peak and the role of excited states. The basis of our speculation is an interaction potential computed by Kokh *et al.* for N(⁴S) and N(²D), the result of which is shown in figure 6 [65].

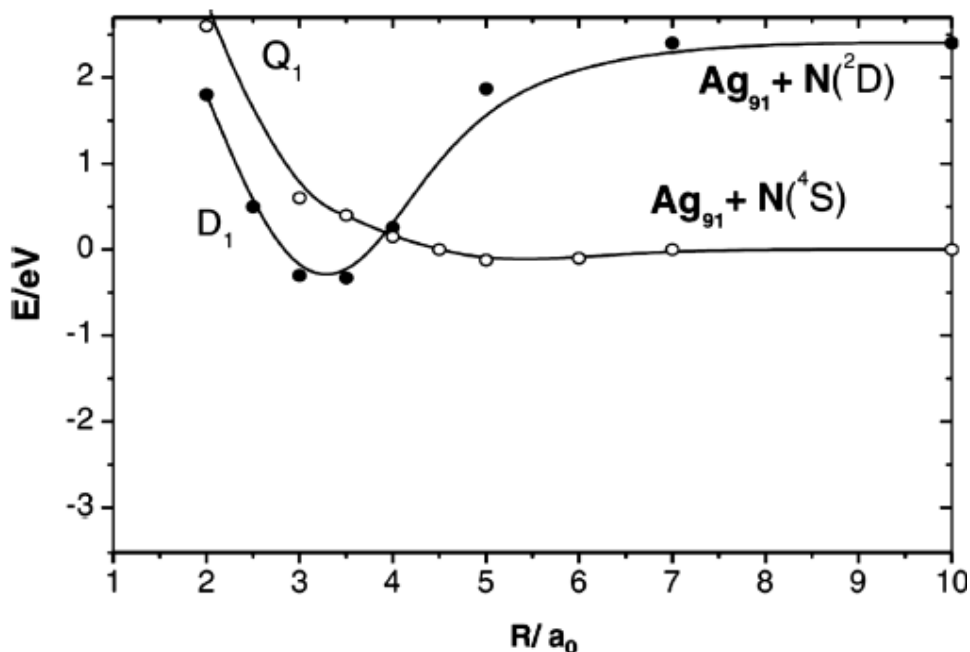


Figure 6: Reactive atom-surface potential energy curves for the ground state N (⁴s) and excited state N (²D) interacting with Ag₉₁ clusters (Reproduced from Ref. [65]).

The two potential curves shown are for systems with a quartet N-atom and with a doublet N-atom. The doublet surface shows a small well, while the quartet surface is essentially purely repulsive. If we assume that there are no interactions between the two states, in other words that the spin of the N-atom does not flip during interaction with the Ag, we see that indeed there is a chemisorption-like system involving N(²D) and an inert, Ar-like potential for N(⁴S). This would imply that most of the scattering of the ground state atoms should be Ar like. This is clearly incorrect, because the relative reflection intensity at specular is much lower (factor 25-50) than for the Ar case even though the ground-state is the dominant component in the incident beam. A second assumption could be that the interaction between these two potentials is extremely strong. This implies that the adiabatic ground state surface has a deep well. In fact, later DFT calculations show in figure 4 that the well in the D₁ curve is not deep enough [60]. By extension, the potential for the excited state atoms would not have a deep well close to

the surface, leading to much less corrugation in the excited state potential. In this case the data in figure 3 can be explained. Ground state N scatters adiabatically from the surface and feels the deep chemisorption well. Excited state N scatters from a potential that is much less corrugated and this leads to Ar-like scattering and a narrow specular peak.

The discussion above heavily borrows ideas from gas phase scattering involving electronic transitions [66]. For instance, collisions like $\text{Na} + \text{I} \rightarrow \text{Na}^+ + \text{I}^-$ can be described by interactions along two distinct interaction potential curves with a well-defined avoided crossing [67]. In the present case the situation is much more complex, because at surfaces distinct electronic states evolve into continua of states and the interactions between these states is very complex [24-26, 68].

In addition to the angular intensity distributions, information on the dynamics of the gas-surface interaction can also be obtained from a measurement of the energy transfer in the collision utilizing time-of-flight techniques. If the resulting spectra are represented by shifted Maxwell Boltzmann distributions, they can be characterized quite well by a single number: the final average energy after the collision. This quantity is plotted in reduced form in figure 7, which shows data for two angles of incidence: $\Theta_i = 40^\circ$ and 60° .

The relative energy transfer E_f/E_i is plotted as a function of the total scattering angle. In the case that the energy transfer is determined in a single collision with a single surface atom, then the energy transfer is determined by Θ_t . The expected energy transfer computed based on the binary collision model is plotted as a dotted line in figure 7. The experimental data for two angles of incidence nicely superimpose on this plot. The data follows the binary collision model very well. Clearly, the energy transfer is mainly determined in a single collision with an individual surface atom. This in turn is consistent with the observed large corrugation of the potential surface. Large corrugation exposes the individual atoms very well. As the energies involved in the collision are far above thermal the influence of T_s on E_f/E_i is small (see [51]).

The most surprising observation in the data is that of an apparent energy gain at small Θ_t . At $\Theta_t=40^\circ$ $E_f \approx 1.5 \cdot E_i$ implying an energy gain around 2 eV. This is extremely unlikely since the only additional energy available is thermal motion of the surface. In fact it is more probably that this effect is a result of the very broad thermal spread of the N-atom beam. If the angular width for scattered atoms increases with energy, scattering to $\Theta_t=40^\circ$ may be limited to the faster particles in the beam. In that case the calculation of E_f/E_i is no longer straightforward because one needs to know the average E_i of the subset of atoms belonging to those specific scattering conditions. This will be higher than the $\langle E_i \rangle$ of the direct beam since atoms with low E_i simply will not scatter over the full

angular range. A specific calculation based upon the experimental data is not possible if the energy dependence of the angular distribution has not been measured with narrow energy distributions. However, using classical dynamics simulations the effect can be examined rather easily, which has been done by Marton-Gondre *et al.* [69]. These authors found an energy transfer that matches the experimental results and the binary collision model rather closely. At lower Θ_t an upwards deviation of E_f/E_i is also observed in the case of an effusive beam, which is attributed to an effect as sketched above. It should be noted that in calculations for mono-energetic beams the sharp increase with decreasing Θ_t is not observed and E_f/E_i remains at or below the binary collision curve at all Θ_t .

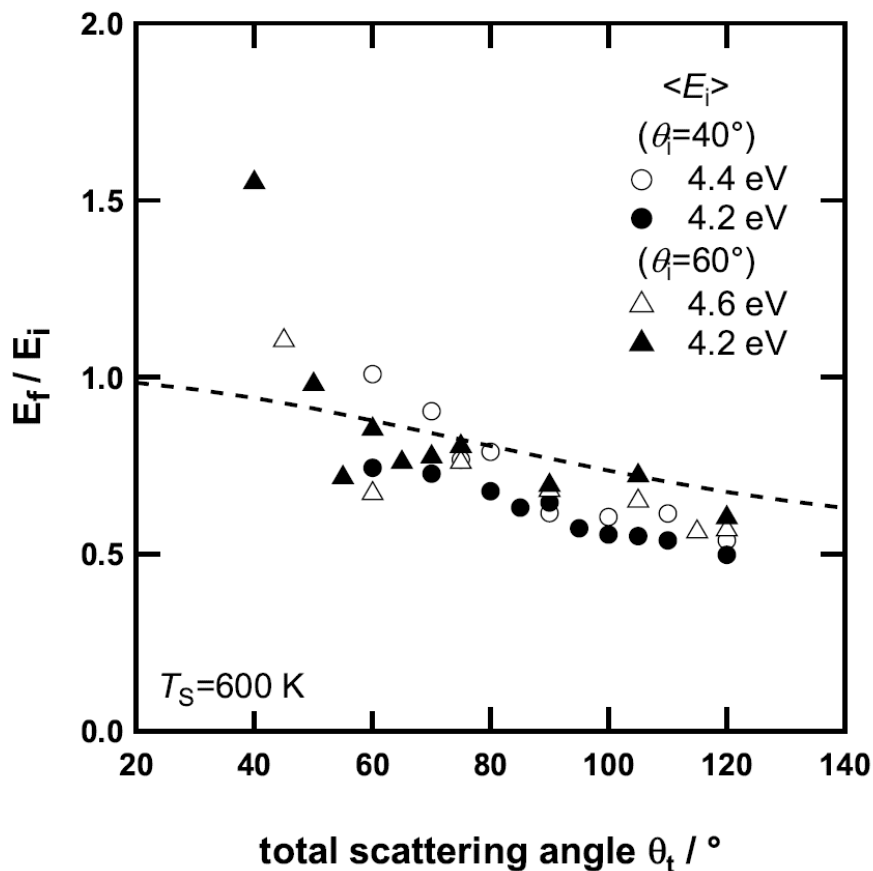


Figure 7: Ratio of final energy to initial energy of N atoms scattered from Ag(111) for incident angles of 40° and 60°.

N-atom scattering at N-covered Ag(111)

Dropping the surface temperature to $T_s=300$ K while exposing a bare Ag(111) sample to the nitrogen plasma beam results in the surface becoming covered by N-atoms. Even though the N-atom beam energy is rather high, post irradiation TPD measurements confirm increasing N-atom adsorption with exposure time, leading to eventual saturation. The N₂ desorption peak occurs at 430K, in agreement with earlier measurements by Carter *et al.* [37]. The structure of the N-covered Ag(111) surface is not very well known. By analogy to other systems and following the calculations by Martin-Gondre *et al.* we assume that the N-atoms reside in the hollow sites. Most likely, every other hollow site will be empty. The bonding distance between the N-atoms and the plane through the outermost Ag nuclei is 0.1 nm, meaning that the N-atoms are almost absorbed into the Ag lattice.

Scattering N-atoms from such an N-covered Ag(111) surface at $\Theta_i=60^\circ$ yields an angular intensity distribution such as is shown in figure 8. The corresponding angular distribution from the “bare” surface at $T_s=500$ K is also shown. The result is quite remarkable because there is very little change between scattering from the bare surface and from the N-atom covered surface. There is slightly more specular scattering in the peak, while the amount of back scattering to the surface normal is decreased for the N-covered surface. The energy transfer in scattering from the N-covered surface (not shown) is essentially undistinguishable from that for scattering from the bare surface (figure 7). Obviously most of the scattering is unchanged indicating that the adsorbed N-atom does not significantly alter the interaction potential, and certainly not that of the unfilled three-fold hollow site. The data suggests that the potential for the filled site is also fairly similar, and hence the corrugation remains large. It is important to note that the relative reflection intensity remains unchanged, as is clear from figure 8, excluding the possibility of loss of a significant amount of the incident N flux, for instance by sticking.

From the close correspondence between N-atom scattering patterns we infer that the deep chemisorption well is not passivated by the adsorbed N-atom. The reason for this might be that the strong Ag-N attraction is replaced by a similarly strong N-N attraction. We note that the onset of repulsive forces between Ar and Ag(111) at the threefold hollow site occurs at about 0.2 nm [63]. For N-atoms interacting with this hollow site the value is more like 0.1 nm. This very close approach is due to the strong attraction. If adsorbing an N-atom would make the local interaction of incident N atoms “Ar/Ag-like”, then half of the unit cell would become uncorrugated resulting in a dramatically increased specular intensity. This is inconsistent with the measurements,

which shows a specular intensity that is very similar to the bare surface. It seems likely that thanks to the N-N attraction the effective overall potential between N-atoms and the (N-) Ag(111) surface does not change much. This conjecture could be tested by measurements of Ar scattering from N-Ag(111), which are in preparation.

Passivation of part of the unit cell has been observed earlier by Berenbak *et al.* for the scattering of NO from H-covered Ru [70, 71]. In that case half of the unit cell was passivated by hydrogen resulting in a spectacular increase in very sharp specular scattering. However, the other half of the unit cell remained reactive as the sticking coefficient for NO dropped to only 50% and not to 0%. These results demonstrate that passivation can dramatically alter angular distributions. By analogy they suggest that for N-atoms the Ag(111) surface is not passivated by pre-adsorbed N-atoms.

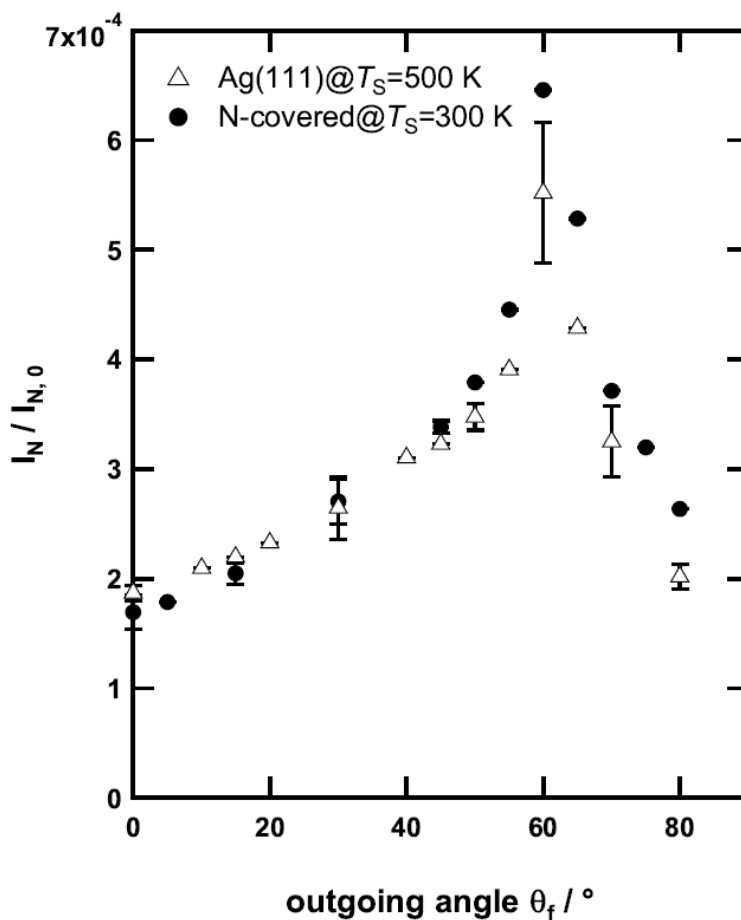


Figure 8: Comparison of the N-atom angular distribution for N atoms scattering from bare and N-covered Ag(111). The incidence angle is 60°.

The sharp peak in the angular distribution for scattering of N-atoms from the bare Ag(111) surface has been attributed to the presence of excited doublet N-atoms in the beam. If this is the case, the electronic transitions (or absence thereof) for the excited N-atoms are not changed by the presence of adsorbed N-atoms. In conclusion we feel the interpretation of the angular scattering data suggests that the interaction dynamics at clean and N-covered surface does not change and that coverage of an Ag(111) surface by N-atoms does not remove the strong corrugation of the interaction potential.

N₂ scattering and formation at N-Ag(111)

The relative angular intensity distribution for scattering of N₂ at $\Theta_i=60^\circ$ from bare Ag(111) ($T_s=500$ K) and N-covered Ag(111) ($T_s=300$ K) are plotted in figure 9 [55]. A very sharp specular peak is observed with a very high relative angular intensity (≈ 0.02), which is significantly higher than that observed for Ar (≈ 0.012 ; see figure 3(a)).

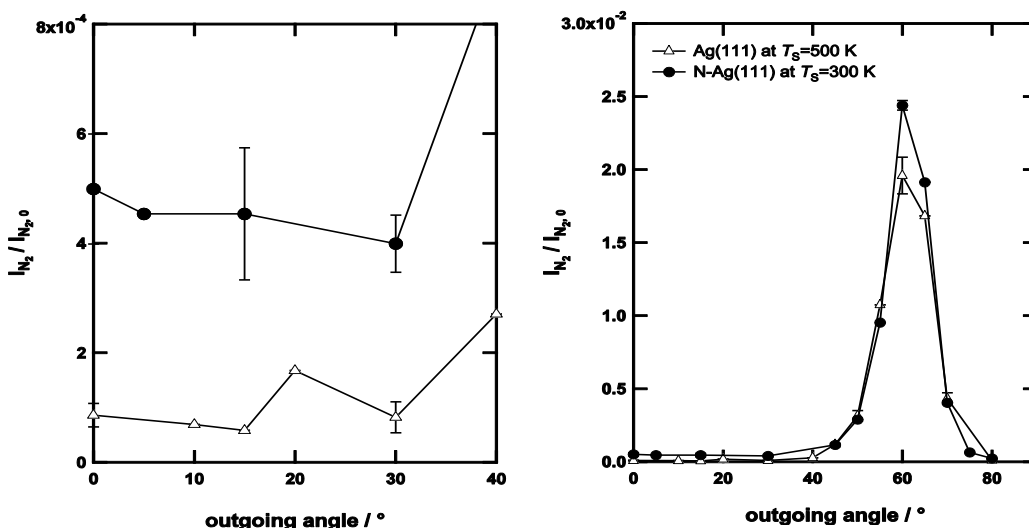


Figure 9: Angular intensity distributions of N₂ scattered for bare and N-covered Ag(111). The left-hand-side panel is a blow-up of the small outgoing angle region of the right-hand-side panel.

Clearly the surface is completely inert and lacks corrugation toward N₂. The adsorbed N-atoms do not seem to play a major role. Presumably, this is because the N-atoms are positioned at a depth of only 0.1 nm above the surface plane of Ag atoms where they are largely invisible for the incident N₂. However, a careful inspection shows that there is additional N₂ signal at the surface normal in the case of the N-covered surface, which is absent for the bare surface. There can be various explanations for this signal. One is that it is due to the increased roughness of the surface. If this is the case

Ueta *et al.* [55] argue that it should result in a broadening of the specular peak at both sides. This is not the case, in particular at $\Theta_i=80^\circ$ where other measurements for corrugated systems, for instance N-atom scattering!, do show significant signal. By contrast, the signal for N₂ at $\Theta_i=0^\circ$ has a higher relative angular intensity (≈ 0.0005), than that for N-atoms at the same angle (≈ 0.0002). This analysis suggests that this N₂ signal is not due to scattering of N₂ from the beam.

An alternative explanation for the N₂ signal is that it is due to a pick-up reaction of a surface N-atom by a fast incident N-atom. This would be an Eley-Rideal reaction or a hot atom reaction [72, 73]. A detailed analysis of the energies of the N₂ formed should shed more light on this. This analysis has been carried out and will not be discussed in detail. Summarizing, it was found that a consistent fit of all N₂ time-of-flight data could not be obtained on the basis of a single shifted Maxwell Boltzmann distribution, although a reasonable fit for a subset of the angular data, specifically the region around the surface normal, could be obtained in this way. However, good fits to all angular time-of-flight data could only be obtained using a combination of a slow and a fast N₂ component. Note that this slow component is faster than the Maxwell distribution representing thermalization at the surface. In this case, angular intensity and energy distributions can be derived from the TOF data under two broad assumptions: either that the N₂ signal at the normal is due to incident N reacting with an adsorbed N-atom or that it is due to N₂ scattering. The results of the two component fits derived on the basis of these assumptions are shown in figure 10.

A good fit for the angular distributions can be obtained on the basis of both incident N (top panels) and N₂ (bottom panels). However, for incident N₂-molecules the N₂ observed along the normal have energies of 2.0 and 9.0 eV. The latter is unphysical since it is extremely unlikely that N₂-molecules gain ~ 4 eV in a fast collision with an Ag(111) surface. For incident N-atoms, the N₂ observed at the normal have energies of 1.5 and 5.5 eV. Since the bond energy of N-N is 9.8 eV, its binding energy to the surface close to zero, the atomic binding energy is around 2 eV according to DFT [60] (shown in figure 4) and the N-translational energy more than 4 eV, it is clear that recombinative desorption can without any problem lead to the energies observed. The fast N₂ can be attributed to an Eley-Rideal or hot atom reaction and the slow N₂ to recombinative desorption of accommodated N-atoms.

If indeed an Eley-Rideal like process is being observed it would be the first time for such a reaction for a non-hydrogenic system. Eley-Rideal reactions have been observed for the pick-up of hydrogen by fast projectiles such as the DABCO molecule, Cl atoms, hydrogen atoms and, as is shown later, O atoms [74-77]. Although the evidence

seems to point to such a process a definitive experimental proof has not been given and this is a topic for future research in our laboratory. Also theoretical analysis of the present data could lead to a convincing proof of the mechanism.

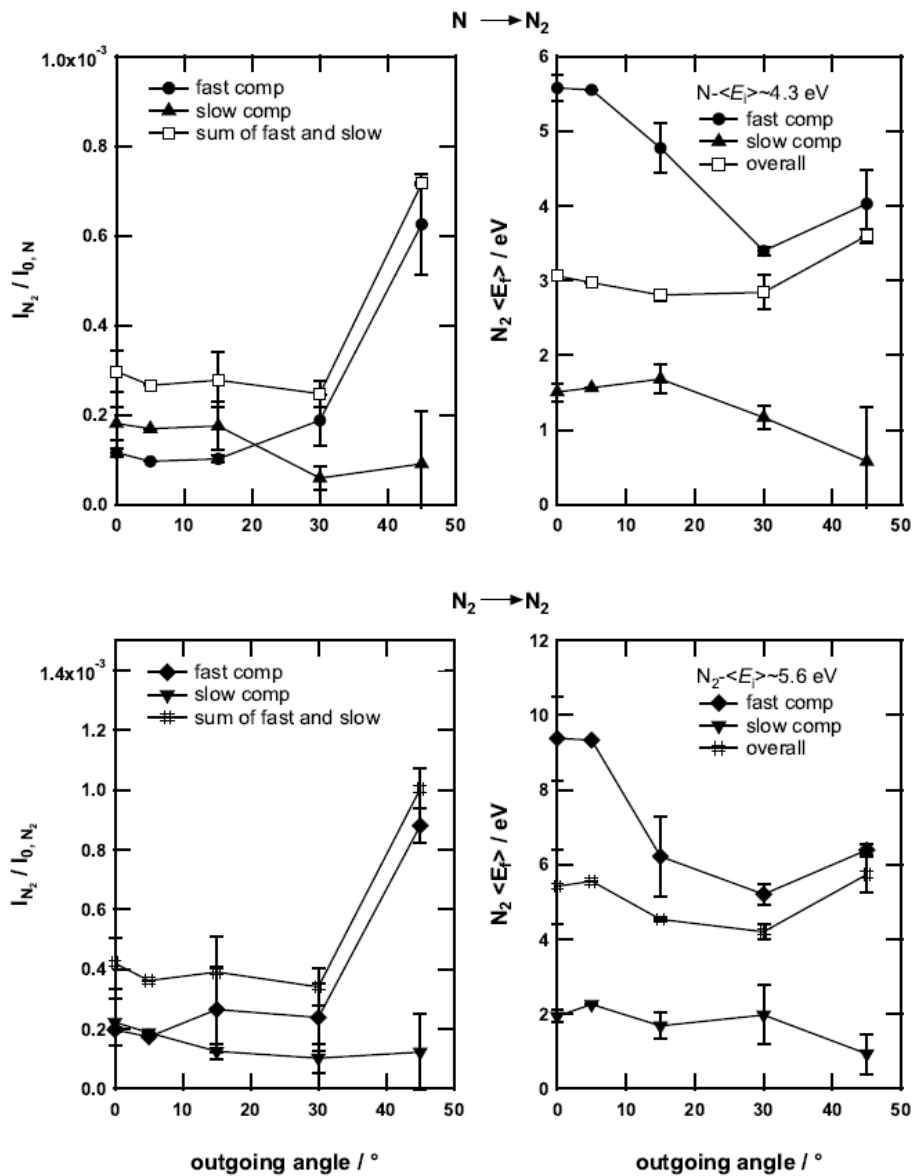


Figure 10: Results of two component fitting to near-normal N₂ TOF data collected for N₂ scattering from N-covered Ag(111). The top two panels show the intensity and energy distributions derived based on an assumption of a pick-up reaction involving incident N atoms. The bottom two panels show the corresponding distributions derived based on the assumption of scattering of incident N₂ molecules.

Note that the similarity between both the scattered N-atom intensities (see figure 8) and energy distributions (not shown) from bare and N-covered Ag(111) is compatible with a pick-up reaction, which requires an attractive interaction between incident and adsorbed N atoms. We have argued that the pre-adsorption of N atoms does not dramatically alter the attractiveness of the site because the attractive potential of the vacant three-fold hollow site is replaced by an attractive interaction between the adsorbed and incident N atoms that is of comparable magnitude. In some instances, the inter-atomic interaction will be sufficient to overcome the chemisorption energy and recombinative abstraction can occur.

N and N₂ scattering at N-Ru(0001)

All work described above has been carried out for the Ag(111) surface, typically a very unreactive surface, that only weakly binds N-atoms. The Ru(0001) surface is much more reactive. For instance, Ru can be used to activate N₂ for ammonia synthesis. Nevertheless, dissociative chemisorption of N₂ on Ru(0001) is a highly activated process, see e.g. [32, 33]. Only at beam energies above 3 eV does the N₂ dissociative sticking coefficient rise above 1%. Below that energy Ru is very inert to N₂ and angular distributions for N₂ scattering resemble those for noble gases and that for N₂ scattering at Ag(111). Papageorgopoulos *et al.* have demonstrated that the width of the angular distribution $\Delta\Theta_f$ for N₂ scattering from Ru(0001) first decreases with increasing energy and later starts to rise again [78]. These results are reproduced in figure 11.

Also shown in this figure are the results from classical trajectory calculations by Díaz *et al.* [32]. The calculations match the experimental results rather well and indicate that the initial decrease of $\Delta\Theta_f$ is due to a decrease in parallel momentum transfer. Previously, the decrease was attributed to thermal scattering [78]. The subsequent increase in $\Delta\Theta_f$ is attributed to the increase in corrugation of the potential with increasing energy. Please note that $\Delta\Theta_f$ at $E_i=2$ eV is twice that for N₂ scattering at Ag(111) at 5 eV! From potential energy surfaces for the system published by Diaz *et al.* it is clear why this is so. Above 2 eV the barrier for dissociative chemisorption of N₂ is approached and the surface becomes much more corrugated as a consequence. Preliminary data from our lab on the angular distribution for N₂ and N scattering from an N-covered Ru(0001) surface show that at higher collision energies the angular distributions differ dramatically. This is illustrated in figure 12.

The angular distribution for N₂ scattering at an incidence angle of 60° from N-Ru(0001) is very broad, while still showing most scattered signal around the specular angle. $\Delta\Theta_f$ is more than twice the value at $E_i=2$ eV in figure 11 suggesting that N₂ has

become very reactive at 5 eV or that the N-adatoms introduce significant surface roughening.

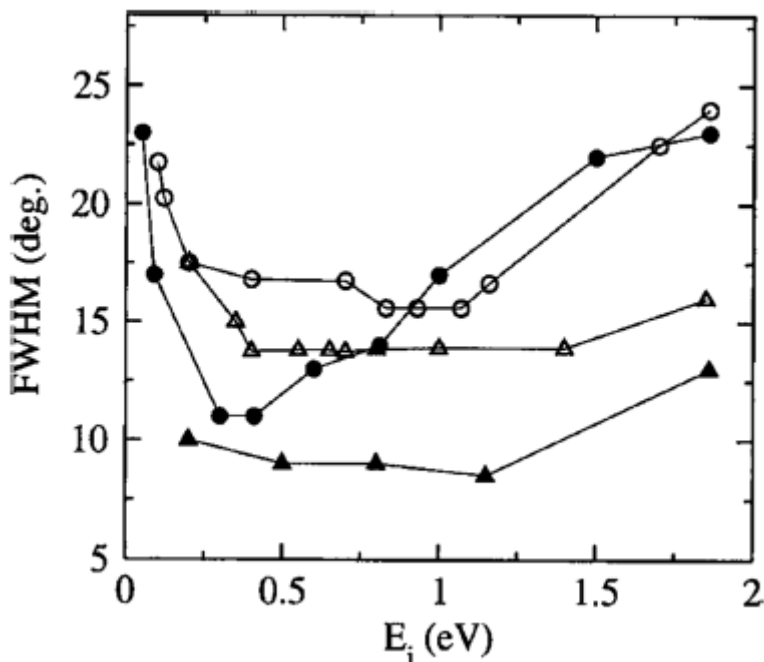


Figure 11: Angular width of N₂ scattering from Ru(0001) as a function of incident particle energy. Open and filled symbols correspond to experimental data and theoretical results respectively. Circles $\Theta_i=40^\circ$ and triangles $\Theta_i=50^\circ$.

The angular distribution for N-atom scattering shown in Fig. 14.12 also demonstrates a strong chemical interaction between N-atoms and the N-Ru(0001) surface. It is less broad than that for N₂ scattering. Note however that it is shifted to super-specular angles. Furthermore, although its angular distribution is narrower than that for N atoms scattering from bare/N-covered Ag(111) (see figure 8), the relative N intensity is lower as indicated by the respective Y-scales. Under the assumption that full integration of all scattered N, both in- and out- of plane, in the case of figure 8 would be sufficient to account for (almost) all incident N atoms, then the N atom angular distribution shown in Figure 12 suggests that a significant fraction of those N atoms are missing in the case of the N-covered Ru(0001) surface. The implication of this is that the missing N atoms are recombining at the surface and are perhaps emerging as part of the very broad N₂ distribution, which has a relative intensity that is a factor of 20 higher than that of the scattered N atoms. Since there is very little intensity at the surface normal, most of this recombination has to proceed via an Eley-Rideal mechanism.

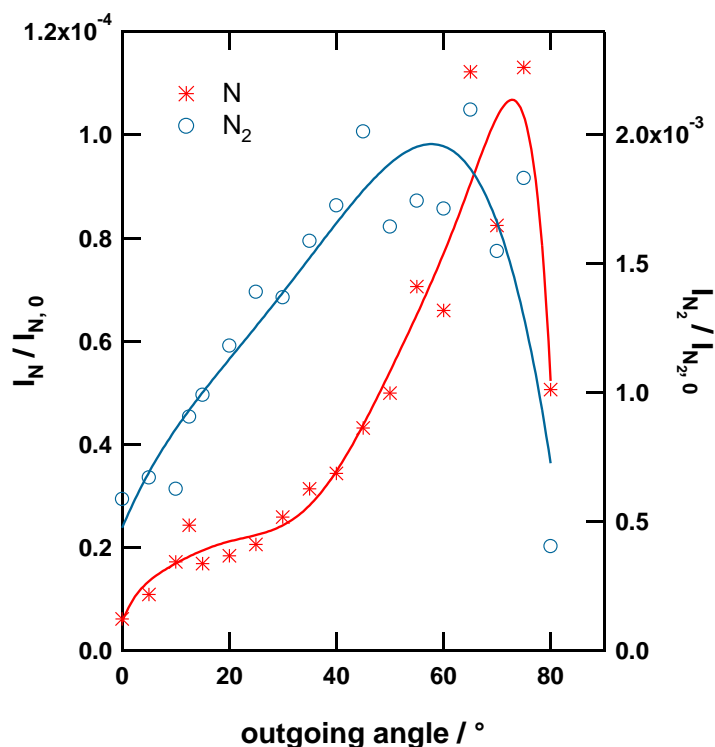


Figure 12: Relative intensity distributions for N and N₂ scattering from N-covered Ru(0001)

Although further detailed experiment are needed, by comparing N and N₂ intensities and width of angular distribution from N-covered Ru(0001) with those of (N-covered) Ag(111), it is demonstrated that the Ru surface is not passivated by adsorbed N atoms and remains highly reactive.

Other systems

Scattering of hypersonic N-atoms from solid surfaces has only very rarely been studied. Some other radical atoms, such as F, O, and H, have been investigated a little more frequently as introduced earlier in this chapter. This literature will not be reviewed here.. As a single example we show results for O-atom scattering from a saturated hydrocarbon liquid surface in figure 13 [79].

The beam is produced in a laser detonation source and has an energy of about 5 eV. At first it is clear that in this case also specular reflection from the surface is observed. Even though the liquid surface is much more dynamic than a metallic single crystal, the sudden collision event is reminiscent of scattering from metals. About 50% of the initial beam energy is retained while the mass of the individual target atoms is much

lower than that of Ag or Ru. A more detailed analysis of the time-of-flight spectra of the scattered particles shows that this distribution can be decomposed in two parts, a slow and a fast distribution. The O-atom scattering also demonstrates the occurrence of Eley-Rideal reactions. The angular and velocity distributions of OH formed in collisions of O atoms with the liquid hydrocarbon surface are identical to those for the O-atoms. The pick-up of an H-atom from the surface does not significantly change the O-atom velocity which is very reasonable in view of the very different masses of O and H. The dynamics of a reaction of N + N_{ad} would be very different because of the different mass ratio.

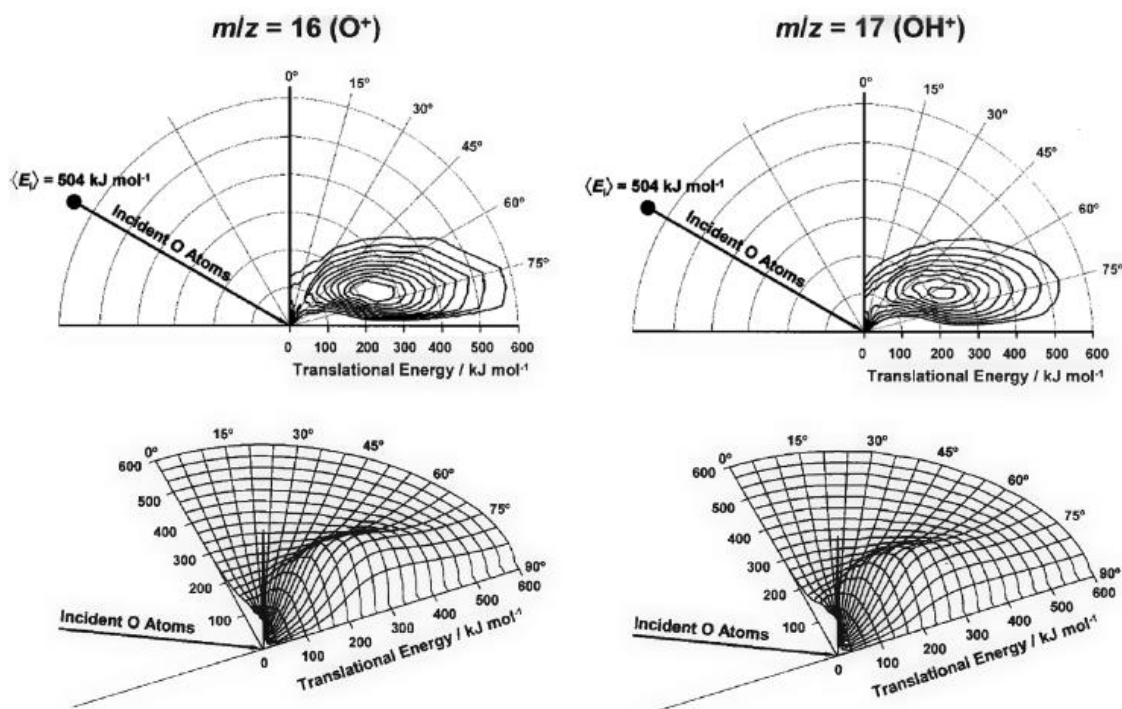


Figure 13: Reproduction of scattered O and OH translational energy distributions from squalane. Plotted as contours and in a 3D representation are the angular and final energy dependence of the scattered intensity for O (left) and OH right. (Reproduced from Ref. [79].)

Conclusions

Molecular beam scattering of fast radical atoms from surfaces is a unique tool to investigate the dynamics of the interaction and for the study of the onset of chemical reactions at surfaces. From the material presented we conclude that the interaction of radical atoms is dominated by deep attractive potentials, leading to large corrugation and very broad angular distributions from structure scattering. We note that adsorbed N-atoms do not significantly change the angular distributions of N atoms scattered from Ag(111) and that Ag and Ru surfaces are not passivated by adsorbed N-atoms. We have demonstrated strong evidence for an important role of electronic excitation of the N-atoms, although further work on the composition of the beam is clearly needed. Finally, we note that Eley-Rideal reactions between incident and adsorbed N-atoms on Ag(111) and Ru(0001) may be occurring.

Acknowledgements

This work is part of the research programme of FOM and is supported financially by NWO. Valuable discussions with Ludovic Martin-Gondre, Maria Blanco-Rey, Inaki Juaristi, Ricardo Diez Muino and Geert Jan Kroes are gratefully acknowledged.

References

1. F. O. Goodman and H. Y. Wachman, *Dynamics of Gas-Surface Scattering*. 1976, New York: Academic press.
2. J. A. Barker and D. J. Auerbach, *Gas-surface interactions and dynamics: thermal energy atomic and molecular beam studies*. Surface Science Reports, 1984. **4**(1/2): p. 1-100.
3. A. W. Kleyn, *Molecular beam scattering at metal surfaces*, in *Surface Dynamics*, D.P. Woodruff, Editor. 2003, Elsevier: Amsterdam. p. 79-108.
4. A. W. Kleyn, "Basic Mechanisms in Atom-Surface Interactions", in *Handbook of Surface Science, Volume 3: Dynamics*, E. Hasselbrink and B. Lundquist, Editors. 2008, Elsevier: Amsterdam. p. 29-52.
5. A. W. Kleyn and T. C. M. Horn, *Rainbow scattering from solid surfaces*. Physics Reports, 1991. **199**: p. 191-230.
6. J. Los and J. J. C. Geerlings, *Charge exchange in atom-surface collisions*. Physics Reports, 1990. **190**(3): p. 133-190.
7. M. J. Gordon, et al., *Gas-Surface Chemical Reactions at High Collision Energies?* Journal of the American Chemical Society, 2009. **131**(5): p. 1927-1930.
8. H. Winter, *Scattering of atoms and ions from insulator surfaces*. Progress in Surface Science, 2000. **63**(7-8): p. 177-247.

9. H. Winter, *Collisions of atoms and ions with surfaces under grazing incidence*. Physics Reports-Review Section of Physics Letters, 2002. **367**(5): p. 387-582.
10. H. Winter and A. Schüller, *Fast atom diffraction during grazing scattering from surfaces*. Progress in Surface Science, 2011. **86**(9–10): p. 169-221.
11. K. D. Gibson, et al., *Hyperthermal Ar atom scattering from a C(0001) surface*. Journal of Chemical Physics, 2008. **128**(22): p. 224708.
12. T. K. Minton, K. P. Giapis, and T. Moore, *Inelastic scattering dynamics of hyperthermal fluorine atoms on a fluorinated silicon surface*. Journal of Physical Chemistry A, 1997. **101**(36): p. 6549-6555.
13. Z. Shpilman, et al., *Resistance of diamond (100) to hyperthermal atomic oxygen attack*. Applied Physics Letters, 2009. **95**(17): p. 174106.
14. C. Linsmeier, M. Reinelt, and K. Schmid, *Surface chemistry of first wall materials - From fundamental data to modeling*. Journal of Nuclear Materials, 2011. **415**(1): p. S212-S218.
15. K. Schmid, et al., *Interaction of nitrogen plasmas with tungsten*. Nuclear Fusion, 2010. **50**(2): p. 8.
16. H. Tsurumaki, et al., *Optical second-harmonic generation study of incorporation of nitrogen atoms at Si(100) surfaces*. Surface Science, 2007. **601**(19): p. 4629-4635.
17. M. Alagia, et al., *Magnetic analysis of supersonic beams of atomic oxygen, nitrogen, and chlorine generated from a radio-frequency discharge*. Israel Journal of Chemistry, 1997. **37**(4): p. 329-342.
18. S. N. Foner and R. L. Hudson, *Mass Spectrometric Studies of Metastable Nitrogen Atoms and Molecules in Active Nitrogen*. Journal of Chemical Physics, 1962. **37**(8): p. 1662.
19. C.-L. Lin and F. Kaufman, *Reactions of Metastable Nitrogen Atoms*. Journal of Chemical Physics, 1971. **55**: p. 3760.
20. Grecea, M.L., et al., *Co-adsorption of NH(3) and SO(2) on quartz(0001): Formation of a stabilized complex*. Chemical Physics Letters, 2011. **511**(4-6): p. 270-276.
21. H. Nienhaus, *Electronic excitations by chemical reactions on metal surfaces*. Surface Science Reports, 2002. **45**(1–2): p. 1-78.
22. A. M. Wodtke, D. Matsiev, and D. J. Auerbach, *Energy transfer and chemical dynamics at solid surfaces: The special role of charge transfer*. Progress in Surface Science, 2008. **83**(3): p. 167-214.
23. A. M. Wodtke, J. C. Tully, and D. J. Auerbach, *Electronically non-adiabatic interactions of molecules at metal surfaces: Can we trust the Born–Oppenheimer approximation for surface chemistry?* International Reviews in Physical Chemistry, 2004. **23**(4): p. 513-539.
24. S. Roy, N. Shenvi, and J. C. Tully, *Dynamics of Open-Shell Species at Metal Surfaces*. Journal of Physical Chemistry C, 2009. **113**(37): p. 16311-16320.
25. N. Shenvi, S. Roy, and J. C. Tully, *Nonadiabatic dynamics at metal surfaces: Independent-electron surface hopping*. Journal of Chemical Physics, 2009. **130**(17): p. 174107.
26. N. Shenvi, S. Roy, and J. C. Tully, *Dynamical Steering and Electronic Excitation in NO Scattering from a Gold Surface*. Science, 2009. **326**(5954): p. 829-832.
27. M. Alducin, et al., *Why N-2 molecules with thermal energy abundantly dissociate on W(100) and not on W(110)*. Physical Review Letters, 2006. **97**(5): p. 056102.
28. M. Alducin, et al., *Low sticking probability in the nonactivated dissociation of N-2 molecules on W(110)*. Journal of Chemical Physics, 2006. **125**(14): p. 144705.
29. M. Alducin, et al., *Dissociative adsorption of N-2 on W(110): Theoretical study of the dependence on the incidence angle*. Surface Science, 2007. **601**(18): p. 3726-3730.

30. H. Ambaye and J. R. Manson, *Calculations of scattering of N-2 molecules from Ru(0001)*. Journal of Chemical Physics, 2006. **125**(17): p. 176101.
31. C. Diaz, A. Perrier, and G. J. Kroes, *Associative desorption of N-2 from Ru(0001): A computational study*. Chemical Physics Letters, 2007. **434**(4-6): p. 231-236.
32. C. Diaz, et al., *Reactive and nonreactive scattering of N-2 from Ru(0001): A six-dimensional adiabatic study*. Journal of Chemical Physics, 2006. **125**(11): p. 114706.
33. C. Diaz, et al., *Multidimensional effects on dissociation of N-2 on Ru(0001)*. Physical Review Letters, 2006. **96**(9): p. 096102.
34. K. R. Geethalakshmi, et al., *Non-reactive scattering of N(2) from the W(110) surface studied with different exchange-correlation functionals*. Physical Chemistry Chemical Physics, 2011. **13**(10): p. 4357-4364.
35. I. Goikoetxea, et al., *Dissipative effects in the dynamics of N(2) on tungsten surfaces*. Journal of Physics-Condensed Matter, 2009. **21**(26): p. 264007.
36. L. Martin-Gondre, et al., *Dynamics simulation of N(2) scattering onto W(100,110) surfaces: A stringent test for the recently developed flexible periodic London-Eyring-Polanyi-Sato potential energy surface*. Journal of Chemical Physics, 2010. **132**(20): p. 11.
37. R. N. Carter, M. J. Murphy, and A. Hodgson, *On the recombinative desorption of N-2 from Ag(111)*. Surface Sci, 1997. **387**(1-3): p. 102-111.
38. M. J. Murphy, J. F. Skelly, and A. Hodgson, *Translational and vibrational energy release in nitrogen recombinative desorption from Cu(111)*. Chem Phys Lett, 1997. **279**(1-2): p. 112-118.
39. M. J. Murphy, J. F. Skelly, and A. Hodgson, *Nitrogen recombination dynamics at Cu(111): Rotational energy release and product angular distributions*. Journal of Chemical Physics, 1998. **109**(9): p. 3619-3628.
40. J. F. Skelly, et al., *Nitrogen induced restructuring of Cu(111) and explosive desorption of N-2*. Surface Science, 1998. **415**(1-2): p. 48-61.
41. K. Jacobi, H. Dietrich, and G. Ertl, *Nitrogen chemistry on ruthenium single-crystal surfaces*. Appl Surf Sci, 1997. **121**: p. 558-561.
42. H. Dietrich, K. Jacobi, and G. Ertl, *Vibrations, coverage, and lateral order of atomic nitrogen and formation of NH₃ on Ru(10(1)over-bar0)*. J Chem Phys, 1997. **106**(22): p. 9313-9319.
43. S. Schwegmann, et al., *The adsorption of atomic nitrogen on Ru(0001): Geometry and energetics*. Chem Phys Lett, 1997. **264**(6): p. 680-686.
44. A. W. Kleyn, *Molecular beams and chemical dynamics at surfaces*. Chemical Society Reviews, 2003. **32**(2): p. 87-95.
45. A. C. Kummel, et al., *Direct inelastic scattering of N₂. IV. Scattering from a high temperature surface*. Journal of Chemical Physics, 1989. **91**: p. 5793-5801.
46. G. O. Sitz, A. C. Kummel, and R. N. Zare, *Alignment and orientation of N₂ scattered from Ag(111)*. Journal of Chemical Physics, 1987. **87**: p. 3247-3249.
47. G. O. Sitz, A. C. Kummel, and R. N. Zare, *Direct inelastic scattering of N₂ from Ag(111). I. Rotational populations and alignment*. Journal of Chemical Physics, 1988. **89**: p. 2558-2571.
48. G. O. Sitz, et al., *Direct inelastic scattering of N₂ from Ag(111). II. Orientation*. Journal of Chemical Physics, 1988. **89**: p. 2572.
49. A. Raukema, *Dynamics of Chemisorption*. 1995, University of Amsterdam: Amsterdam.
50. F. Gou, et al., *A new time-of-flight instrument capable of in situ and real-time studies of plasma-treated surfaces*. Vacuum, 2006. **81**(2): p. 196-201.

51. H. Ueta, M. A. Gleeson, and A. W. Kleyn, *Scattering of Hypertermal Nitrogen Atoms from the Ag(111) Surface*. Journal of Physical Chemistry A, 2009. **113**(52): p. 15092-15099.
52. M. C. M. van de Sanden, et al., *A combined Thomson--Rayleigh scattering diagnostic using an intensified photodiode array*. Review of Scientific Instruments, 1992. **63**(6): p. 3369-3377.
53. R. P. Dahiya, et al., *Dissociative recombination in cascaded arc generated Ar--N[_{sub} 2] and N[_{sub} 2] expanding plasma*. Physics of Plasmas, 1994. **1**(6): p. 2086-2095.
54. A. Raukema, et al., *A three-axis goniometer in an UHV molecular beam experiment*. Measurement Science and Technology, 1997. **8**(3): p. 253.
55. H. Ueta, M. A. Gleeson, and A. W. Kleyn, *The interaction of hypertermal nitrogen with N-covered Ag(111)*. Journal of Chemical Physics, 2011. **135**(7): p. 074702.
56. H. Ueta, M. A. Gleeson, and A. W. Kleyn, *The interaction of hypertermal argon atoms with CO-covered Ru(0001): Scattering and collision-induced desorption*. Journal of Chemical Physics, 2011. **134**(6): p. 064706.
57. H. Ueta, M. A. Gleeson, and A. W. Kleyn, *Scattering of hypertermal argon atoms from clean and D-covered Ru(0001) surfaces*. Journal of Chemical Physics, 2011. **134**(3): p. 034704.
58. K. C. Janda, et al., *Direct measurement of velocity distributions in argon beam--tungsten surface scattering*. The Journal of Chemical Physics, 1980. **72**(4): p. 2403-2410.
59. M. E. M. Spruit, et al., *TRAPPING-DESORPTION OF O-2 FROM AG(111)*. Surface Science, 1989. **215**(3): p. 421-436.
60. L. Martin-Gondre, private communication.
61. B. Berenbak, et al., *Ar scattering on Ru (0001): a comparison to the washboard model*. Physical Chemistry Chemical Physics, 2002. **4**(1): p. 68-74.
62. R. J. W. E. Lahaye, et al., *Out-of-plane scattering of Ar from Ag(111)*. Surface Science, 1996. **363**(1-3): p. 91-99.
63. R. J. W. E. Lahaye, et al., *The scattering of Ar from Ag(111): a molecular dynamics study*. Surface Science, 1995. **338**(1-3): p. 169-182.
64. E. J. J. Kirchner, A. W. Kleyn, and E. J. Baerends, *A comparative study of Ar/ Ag(111) potentials*. Journal of Chemical Physics, 1994. **101**(10): p. 9155-9163.
65. D. B. Kokh, R. J. Buenker, and J. L. Whitten, *Trends in adsorption of open-shell atoms and small molecular fragments on the Ag(111) surface*. Surface Science, 2006. **600**(23): p. 5104-5113.
66. J. Los and A. W. Kleyn, *Ion-pair formation*, in *Alkali halide vapors: Structure, spectra and reaction dynamics*, P. Davidovits and D. L. McFadden, Editors. 1979, Academic Press: New York. p. 275-330.
67. A. W. Kleyn, J. Los, and E. A. Gislason, *Vibronic coupling at intersections of covalent and ionic states*. Physics Reports, 1982. **90**: p. 1-71.
68. J. C. Tully, *Concluding remarks Non-adiabatic effects in chemical dynamics*. Faraday Discussions, 2004. **127**: p. 463-466.
69. L. Martin-Gondre, et al., *Competition between Electron and Phonon Excitations in the Scattering of Nitrogen Atoms and Molecules off Tungsten and Silver Metal Surfaces*. Physical Review Letters, 2012. **108**(9): p. 096101.
70. B. Berenbak, et al., *Impact site-dependent molecular anisotropy: NO scattering from Ru(0001)-(1x1)H*. Chemical Physics, 2004. **301**(2-3): p. 309-313.

71. D. A. Butler, et al., *Elastic scattering in a reactive environment: NO on Ru(0001)-(1x1)H*. Physical Review Letters, 1997. **78**(24): p. 4653-4556.
72. D. D. Eley and E. K. Rideal, *Parahydrogen conversion on tungsten*. Nature, 1940. **146**(3699): p. 401-402.
73. J. Harris and B. Kasemo, *On precursor mechanisms for surface reactions*. Surface Science, 1981. **105**: p. L281-L287.
74. C. T. Rettner and D. J. Auerbach, *Dynamics of the formation of HD from D(H) atoms colliding with H(D)/Cu(111): A model study of an Eley-Rideal reaction*. Surface Science, 1996. **358**(1-3): p. 602-608.
75. E. W. Kuipers, et al., *Surface Molecule Proton Transfer in the Scattering of Hypertermal DABCO from H/Pt(111)*. Surface Science, 1992. **261**(1-3): p. 299-312.
76. C. T. Rettner, *Reaction of an H-atom beam with Cl/Au(111): Dynamics of concurrent Eley-Rideal and Langmuir-Hinshelwood mechanisms*. Journal of Chemical Physics, 1994. **101**(2): p. 1529-1546.
77. C. T. Rettner and D. J. Auerbach, *Dynamics of the Eley-Rideal reaction of D atoms with H atoms adsorbed on Cu(111): Vibrational and rotational state distributions of the HD product*. Physical Review Letters, 1995. **74**(22): p. 4551-4554.
78. D. C. Papageorgopoulos, et al., *A molecular beam study of the scattering and chemisorption dynamics of N-2 on Ru(0001)*. Chemical Physics Letters, 1999. **305**(5-6): p. 401-407.
79. J. M. Zhang, D. J. Garton, and T. K. Minton, *Reactive and inelastic scattering dynamics of hypertermal oxygen atoms on a saturated hydrocarbon surface*. Journal of Chemical Physics, 2002. **117**(13): p. 6239-6251.